

N71-34958

Final Progress Report

CASE FILE
COPY

Contract No. NAS 9 - 9317, Modification No. 1 S

Study of the Modulatory Effects of the
Solar Wind on Galactic Cosmic Rays



T. A. Moss, Ph. D
Department of Physics
Louisiana State University in Shreveport

The following is the context entitled "The Modulation of Galactic Protons by the Solar Wind" of a paper which will appear in the July 15 issue of The Astrophysical Journal. It describes in detail the work completed under this contract.

ABSTRACT

Incorporating a Monte Carlo analysis of a radial magnetic field model for the solar wind, we find, for the quiet Sun: A radius for the solar wind cavity of ~ 5 a.u. is compatible with measured proton spectra. The scattering mean-free-path for galactic protons by magnetic irregularities in the cavity is $L(\text{a.u.}) \sim 0.1r^2(\text{a.u.})P^{3/2}(\text{GeV})$. The unmodulated galactic proton energy spectrum is given by $\Psi(E_K) \sim E_K^{-1.5}$ for $0.1 < E_K < 1.5\text{GeV}$. The net work done upon galactic protons by the solar wind is negligible. The net work done on galactic protons by "energetic" stellar winds can be considerable.

I. INTRODUCTION

The problem of the modulatory effects of the solar wind on galactic cosmic rays has been approached by many authors (see, for example, Parker 1965; Jokipii 1966, 1967; Fisk and Axford 1969), generally by solving the transport problem by means of diffusion approximations. Our approach is

to incorporate the physical phenomena that are believed to influence the transport of cosmic rays into a suitable mathematical model and solve the transport problem through the use of Monte Carlo techniques. Our model takes into account scattering by magnetic irregularities in the solar wind, lateral transport of cosmic rays by random walk of the magnetic field lines, and mirroring by converging field lines.

On the basis of the model developed in the following section, we are able to calculate the solar wind modulated differential galactic proton spectrum and the directional energy flows at any desired point within the solar wind cavity for chosen values of the parameters defining the model and for any assumed form of the unmodulated galactic spectrum. In this paper we report results obtained by varying the parameters defining the solar wind energy, the size of the solar wind cavity, and the magnetic scattering mean-free-path, and by assuming two forms of the unmodulated galactic proton spectrum. By comparison of these results with observations made during solar minimum, we are able to reach some conclusions, appropriate to the time of solar minimum, concerning the real values of the solar wind parameters discussed above, an approximate shape of the unmodulated galactic proton spectrum, and the directional energy flow of the cosmic rays in the solar wind.

II. SOLAR WIND MODEL

Our model assumes a particle wind which moves outward from a non-rotating Sun with constant velocity along radial field lines. These

field lines terminate at the boundary of the solar wind "cavity", which has a radius r_m . Following the ideas of Parker (1958), we assume random turbulence cells which propagate magnetic irregularities outward along the field lines. Also, the field lines may themselves randomly walk (Jokipii and Parker 1969) within the cavity. The magnetic turbulence and randomly walking field lines are effective in scattering cosmic ray particles which enter the cavity. (The effects of the randomly walking field lines are particularly important for particles of higher energy.)

The current hypothesis that solar wind particles travel radially outward from the rotating Sun at constant velocity, and the condition that the field lines are frozen to the wind, lead to the conclusion that the field structure in the solar equatorial plane has the shape of an Archimedes spiral (Parker 1958). The spiral lines diverge somewhat more slowly with increasing distance from the Sun than would radial magnetic field lines. This allows particles to mirror at points deeper in the spiral configuration than they would in a radial configuration. In order to bring the results of our radial field calculations closer to what we might expect for an Archimedes spiral, we place the planets at radial distances which correspond to the actual arclengths along spiral field lines from the Sun to the planets. These arclengths can be obtained from satellite observations, which indicate that the field lines in the ecliptic plane at one a.u. are oriented 45° (Ness and Wilcox 1965) away from the Sun-Earth line. Thus, in our radial model, the "detector" for Earth is placed at 1.15 a.u., and the detector for Venus is placed at 0.78 a.u. instead of 0.72 a.u.

III. MONTE CARLO ANALYSIS

A Monte Carlo history follows a cosmic ray particle from the time it enters the solar wind cavity to the time it leaves the cavity or else impacts the Sun.

Our Monte Carlo history is begun by random selection of a galactic cosmic ray particle which is incident on the solar wind cavity at radius r_m . We assume the integral galactic proton spectrum to be represented by

$$\psi(E) \propto 1/E^{1.5} \quad (1)$$

where $\psi(E)$ is the flux of particles with energy $\geq E$. We can choose any desired range ΔE and sample randomly from that range, weighting the choice of energies within ΔE according to the differential spectrum $d\psi/dE$.

Next, the direction of the incident particle is chosen by random sampling from an isotropic distribution. We then follow the particle's guiding center in the magnetic field between scattering events by making use of the invariant P_{\perp}^2/B , where P_{\perp} is the component of momentum perpendicular to the field and $B \propto r^{-2}$ is the field strength at the radial distance r from the center of the Sun. In addition to scattering, an inward moving particle may reach its mirror point and reflect outward.

Scattering points in the field are determined by random selection on the basis of an assumed mean-free-path. That is, the distance along a field line that a guiding center moves before the particle is scattered is determined statistically. The probability that a particle will scatter in one mean-free-path is taken to be $1 - 1/e$. Our mean-free-path, L , may in

general be a function of the position and momentum of the particle. If we assume L is related to the amplitude of the magnetic power spectrum (Jokipii and Parker 1969) and require the wavelength of the magnetic disturbance to equal approximately the radius of gyration of the particle, we find $L \propto p^{1/2}$ or $L \propto p^{3/2}$ respectively according to which power spectrum (power density $\propto f^{-3/2}$ or $f^{-1/2}$) we choose. Then, if we follow Jokipii and Parker's (1969) arguments concerning random walk of the magnetic field lines, we find diffusion across the field lines increases as r^2 . The mean-free-path for isotropic scattering events may then be taken $L = C r^2 p^{1/2}$ or $L = C r^2 p^{3/2}$, where C is a constant.

The mechanics of a scattering event are described in the rest frame of the solar wind. We assume isotropic scattering in that frame. At the point where the particle is scattered, we first compute the angle between the momentum of the particle and the local magnetic field by

$$\cos \alpha = r(r^2 + R^2)^{-1/2} \cos i \quad (2)$$

where r = radial distance of the particle from the center of the Sun,

R = radius of gyration of the particle,

i = pitch angle of the particle.

We then transform the momentum of the particle from the rest frame of the Sun to the solar wind frame via

$$P'_{\parallel} = \gamma (P_{\parallel} - \beta E_T)$$

$$P'_{\perp} = P_{\perp}$$

where P'_{\parallel} and P'_{\perp} are the parallel and perpendicular components of momentum

in the wind frame, P_{\parallel} and P_{\perp} are the momentum components in the solar frame, E_T is the total particle energy in the solar frame, and β is the ratio of wind velocity to the velocity of light in the solar frame, with $\gamma = (1 - \beta^2)^{-1/2}$. We have taken the outward direction as negative here so that β is a negative quantity in these equations.

If we assume that the mass associated with the magnetic scattering center is infinite compared to the cosmic ray particle mass, only the direction of the momentum of the cosmic ray is changed by scattering in the wind frame, so in this frame the scattering angle is picked by random sampling from an isotropic distribution. The new momentum is then transformed back to the solar frame with the usual Lorentz transformations, and the pitch angle in the solar frame is computed from the angle the momentum makes with the local field using the inverse of equation (2). The new value of P_{\perp}^2/B allows us to follow the guiding center to the next scattering or mirroring event, and so on until the history is completed.

We locate our "detectors" at any points r (in practice, at Earth, Venus, and at r_m) and record each passage of a particle at those points. As a particle passes a detector, we compute its pitch angle from our invariant P_{\perp}^2/B . From the pitch angle we compute the angle made with the local field and record that angle and the magnitude of the momentum. We thus obtain the particle momentum distributions relative to the local field for guiding centers which pass the detector points in both the inward and outward directions.

IV. RESULTS

Using our model, we have studied the effects on the cosmic ray proton spectrum of varying r_m , L and β . Other, better known quantities such as B were assigned physically reasonable values and were not varied in this study. We placed detectors at the corrected positions of Venus and Earth (see Section II) and at the edge of the solar wind cavity. We examined, at these points, the differential spectrum and energy current (the summation of the particle energies each weighted by the cosine of the angle between the particle direction and the magnetic field) as a function of our various parameters.

The ratio of the energy current away from the Sun, J_{out} , to the energy current toward the Sun, J_{in} , at the edge of the solar wind cavity for solar wind velocities in the range 300 - 700 Km/sec (Pathak and Sarabhai 1970) was found to be

$$\frac{J_{out}}{J_{in}} \approx 1$$

for all values of r_m (5 a.u., 21 a.u.) and C (0.01, 0.1, 1.0) that we used. However, for $\beta = 0.8$ (as may be the case for some stars) we obtained

$$\frac{J_{out}}{J_{in}} \geq 3$$

at the cavity edge for all values of r_m and C .

The shapes and intensities of the differential spectra obtained at the detectors were insensitive to variations in solar wind velocities in the

range 300 - 700 Km/sec. Therefore, the following results for differential spectra pertain only to the value 300 Km/sec.

Figure 1 shows the assumed incident differential energy spectrum $E_T^{-2.5}$ and the differential energy spectra obtained at our Earth detector for cavity radii of 5 a.u. and 21 a.u. with $C = 0.1$ and $C = 1.0$. Each curve is normalized such that $\Psi(E_T = 1 \text{ GeV}) = 1$ particle. Each differential spectrum is the result of 4×10^5 histories. The same number of histories were run for $C = 0.01$. However, for this case, so few particles were recorded at the Earth detector that an unreasonably high incident flux would be required to yield observed flux values at the Earth.

Comparing the $C = 0.1$ data to the $C = 1.0$ data for $r_m = 5$ a.u. shows that varying L by an order of magnitude changes the shape of the differential spectrum at the low energy end but does not change the overall proton flux very much, even though the number of scattering events in the $C = 0.1$ case is much larger than in the $C = 1.0$ case. The curves for $C = 0.1$ for both $r_m = 5$ a.u. and $r_m = 21$ a.u. show a hump around 2 GeV, the hump being considerably more pronounced in the $r_m = 5$ a.u. curve. The slopes of the $C = 1.0$ curves increase with decreasing energy down to the lowest energy investigated. If they exhibit a hump at all it must be at very low energy. Comparison of the $r_m = 5$ a.u. data to the $r_m = 21$ a.u. data indicates a change in slope at the higher end of the spectrum as well as flux differences for both values of C .

Figure 2 displays the normalized differential galactic spectrum $E_T^{-2.5}$

and the spectra obtained at the Venus detector. Each detector spectrum is the result of 4×10^5 Monte Carlo histories. Each of the spectra is similar to the corresponding spectrum obtained at the Earth detector, but with more statistical fluctuation apparent, particularly in the $r_m = 21$ a.u. data.

As will be seen later, the value $C = 0.1$ provides the most realistic results. We then compare, in Figure 3, the results for $L = 0.1r_P^{2P^{1/2}}$ and for $L = 0.1r_P^{2P^{3/2}}$. Relative differential proton numbers (for 4×10^5 histories) rather than proton flux are plotted in order to better display the relative shapes between the $r_m = 21$ a.u. spectra and the $r_m = 5$ a.u. spectra. (The spectra shapes are the same for proton numbers and proton flux.) In the $r_m = 5$ a.u. data, the most significant effect is in the low energy region. The $r_m = 21$ a.u. data do not give as pronounced shape to the spectra at low energy, although the statistics for these data are not as good as for the 5 a.u. cases. The "hump" behavior is the same at the Venus detector as at the Earth detector, although the poorer statistics for the Venus results makes this behavior more obscure.

In order to further investigate the proton spectrum shape in the low energy range, we ran a series of Monte Carlo histories for which we assumed the integral galactic proton flux spectrum to be of the form $\Psi(E_K) \propto E_K^{-1.5}$, where E_K is the proton kinetic energy. The range $0.1 \leq E_K$ (GeV) ≤ 1.5 was investigated and is shown in Figure 4. Each Monte Carlo curve represents 4×10^5 histories. Curve I is for $L = 0.1r_P^{2P^{3/2}}$ and $r_m = 5$ a.u., Curve II is for $L = 0.1r_P^{2P^{3/2}}$ and $r_m = 21$ a.u., and Curve III is for $L = 0.1r_P^{2P^{1/2}}$ and $r_m = 5$ a.u. The observationally determined differential proton flux at

or near the solar minima of 1954 and 1965 are represented by Curves A (Neher 1967), B (Ormes and Webber 1967), and C (Fan et al. 1968). The curves are displaced from each other in magnitude in order to facilitate comparison of their relative shapes.

Examination of these spectra shows that Curve I with $L = 0.1r^2P^{3/2}$ and $r_m = 5$ a.u. has a shape which is similar to those of the observational curves. We note also that the curve in Figure 3 which has the same L and r_m , but which was obtained by assuming that the integral galactic proton energy spectrum has the form $E_T^{-1.5}$, has similar shape. However, the peak of the spectrum in Figure 3 is located at $E_K \simeq 0.9 - 1.0$ GeV, while the peak of Curve I, Figure 4 is located at $E_K \simeq 0.2 - 0.3$ GeV. The observational curves of Figure 4 peak at $E_K \simeq 0.3 - 0.5$ GeV.

V. SUMMARY

For the radial field model of the solar wind we find:

(1) The ratio of cosmic ray energy current departing the solar cavity to that entering the cavity (a measure of the overall work done on the cosmic rays by the solar wind) is effectively unity (negligible work done) for what we consider to be a reasonable range of values for β . Only in the case of a very energetic stellar wind does J_{out}/J_{in} significantly exceed unity.

(2) Varying the solar wind cavity radius r_m affects the shape in both the low energy and high energy regions of the spectrum.

Varying C and δ in the expression for the mean scattering distance

$$L = Cr^2P^\delta$$

affects primarily the shape of the low energy region of the differential cosmic ray proton spectrum at the detectors.

The choice

$$\begin{aligned} r_m &= 5 \text{ a.u.} \\ L &= 0.1r^2P^{3/2} \text{ a.u.} \end{aligned}$$

produces a close similarity between the computed spectrum shape and the observed spectrum shape for the quiet Sun. Values for r_m as large as 21 a.u. produce computed spectra shapes which are not similar to observed spectra shapes. We note that Jokipii and Parker's (1969) value for the scattering mean-free-path in the vicinity of one a.u. is compatible with $C = 0.1$.

(3) The peak of the computed spectrum falls closer to the observed peak location if we assume the integral galactic proton spectrum incident on the cavity to be of the form $E_K^{-1.5}$ than if we assume the form $E_T^{-1.5}$, for $0.1 < E_K < 1.5$ GeV.

VI. COMMENTS

Result (1) applies strictly to a spherically symmetric solar wind in which only isotropic scattering takes place. Of course, neither of these conditions may prevail in the actual case, but if there is forward-backward symmetry in scattering, then Result (1) may be valid anyhow.

The combined effects of isotropic scattering, relatively long mean-free-path, and a large value of r_m produce a decrease in slope of the differential proton flux in the high energy region. In the case of $r_m = 21$ a.u., out going particles have some opportunity to scatter back toward the detector before escaping the cavity. The probability that they will be scattered again into the outward direction before they cross the detector is not very large because of their relatively long mean-free-paths, hence they may be counted more than once. These effects enhance the flux of protons crossing the detector in the high energy region. For small r_m , the opportunity for back-scattering is considerably reduced for the higher energy protons but persists for the lower energy protons because of their relatively short mean-free-paths. The protons in the small cavity that have a mean-free-path short enough to allow some opportunity to back-scatter but long enough to come back across the detector before scattering again may be responsible for the difference in the humps in the differential proton flux for the $r_m = 5$ a.u. and $r_m = 21$ a.u. cases.

Variation of C results in only very small overall flux changes in the differential proton spectrum but does affect the shape of the low energy region. Both $C = 1.0$ and $C = 0.1$ allow penetration to the Earth detector by particles down to the lowest energies considered, but only the latter value, coupled to a small value of r_m , has the filtering effect which is observed to occur for the lowest energy particles.

In order for the modulated spectrum to exhibit the observed turnover

at the low energy end, r_m must not be so large that too much scattering takes place before the particles reach the Earth detector. However, C must not be much larger than 0.1 so that, for $P < 1$ GeV, the mean-free-path is short enough to produce filtering out of some of the low energy particles. The $P^{1/2}$ dependence of L , with $C = 0.1$ does not produce a small enough L for $P < 1$ GeV, nor does either $P^{1/2}$ or $P^{3/2}$ for $C = 1.0$.

Our conclusion that r_m is small is consistent with theoretical investigations of, for example, Wang (1970), and observations reported by Barth and Thomas (private communication).

We are indebted to Professor J. L. Modisette for his many suggestions and criticisms of this paper. Also, we wish to gratefully acknowledge useful discussions with Dr. R. L. Golden concerning this topic. We wish to thank _____ for helpful criticisms of this work which have enhanced considerably the presentation and discussion of our results.

This work was supported in part by NASA contract NAS 9-9317.

REFERENCES

- Fan, C. Y., Gloeckler, G., and Simpson, J. A. 1968, Can. J. Phys., 46, 548.
- Fisk, L. A., and Axford, W. I. 1969, J. Geophys. Res., 74, 4973.
- Jokipii, J. R. 1966, Ap. J., 146, 480.
- . 1967, ibid., 149, 405.
- and Parker, E. N. 1969, ibid., 155, 777.
- Neher, H. V. 1967, J. Geophys. Res., 72, 1527.
- Ness, N. F., and Wilcox, J. M. 1965, Science, 148, 1592.
- Ormes, J. F., and Webber, W. R. 1967, in Proc. I.U.P.A.P. 10th Int. Conf. Cosmic Rays, Calgary, Canada, paper MOD-40.
- Parker, E. N. 1958, Ap. J., 128, 664.
- . 1965, Planet. and Space Sci., 13, 9.
- Pathak, P. N., and Sarabhai, V. 1970, ibid., 18, 81.
- Wang, J. R. 1970, Ap. J., 160, 261.

Figure 1. Assumed differential galactic proton flux incident on solar cavity ($\propto E_T^{-2.5}$) and calculated proton fluxes at Earth for two values of cavity size, r_m , and two values of C in $L = Cr_P^{3/2}$.

Figure 2. Same as Figure 1, but at Venus.

Figure 3. Comparison of results at Earth for $L = 0.1r_P^{3/2}$ and $L = 0.1r_P^{1/2}$.

Figure 4. Calculated differential proton fluxes at Earth for assumed differential galactic flux ($\propto E_K^{-2.5}$), compared with observed fluxes at solar minimum. Curve parameters are given in text.

Figure 1

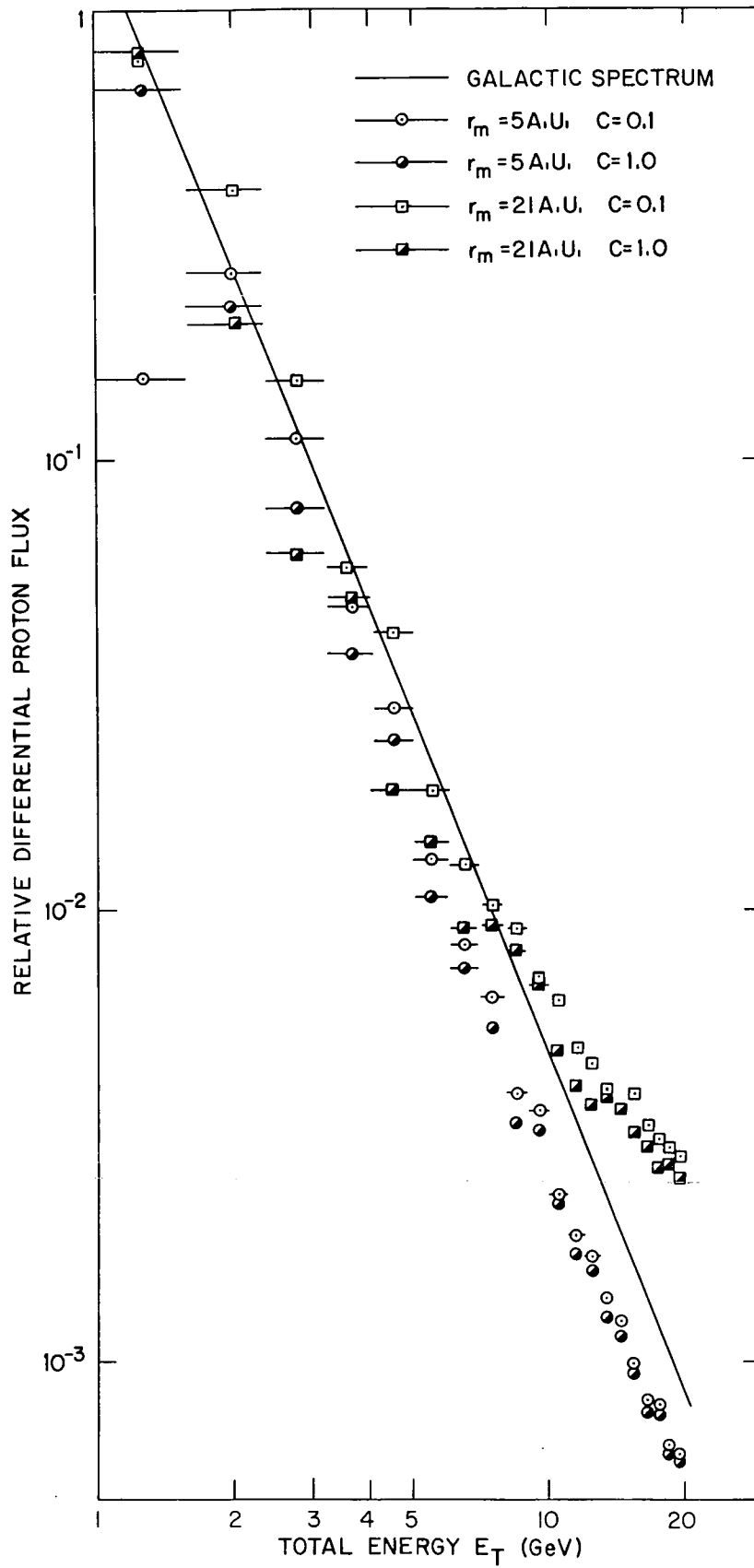


Figure 2

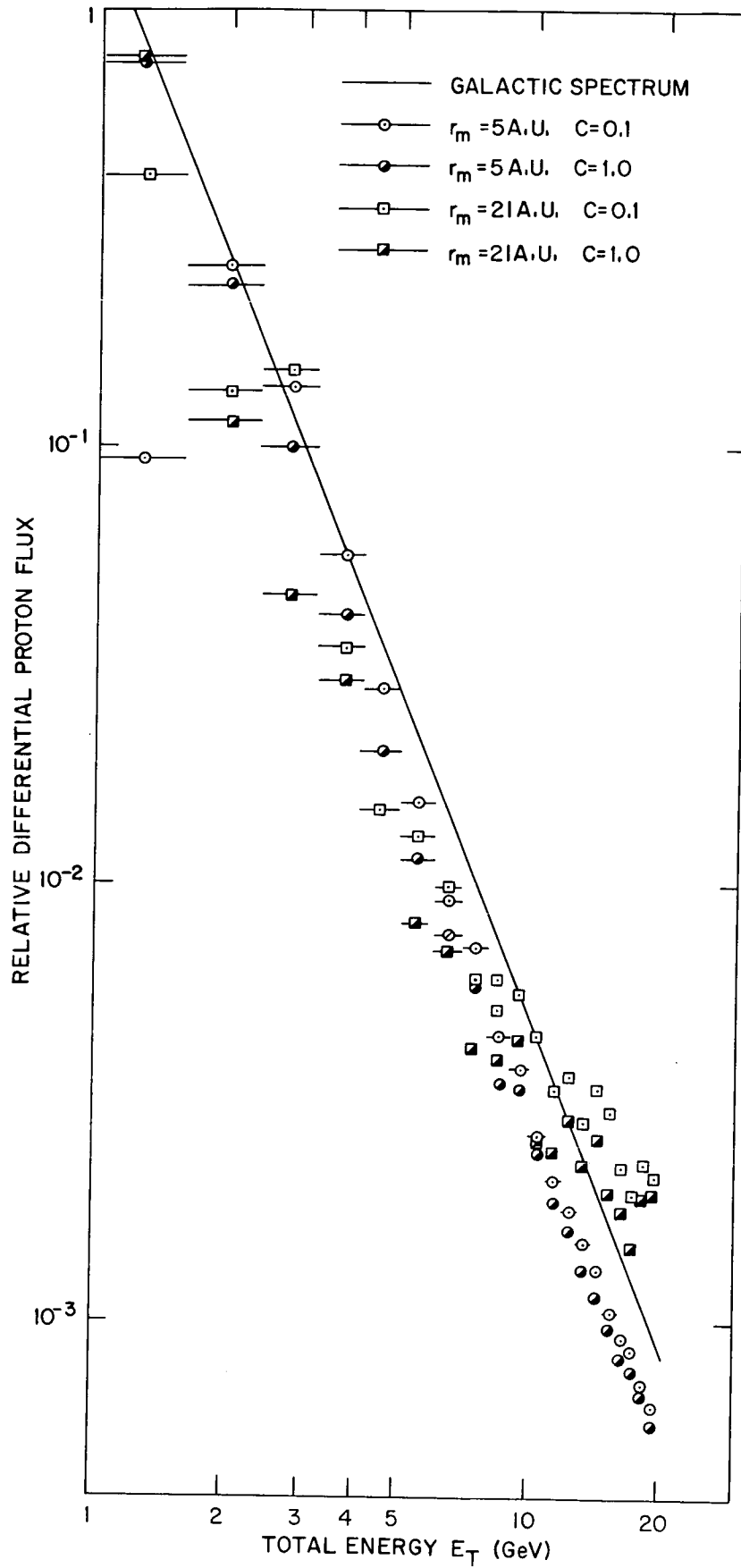


Figure 3

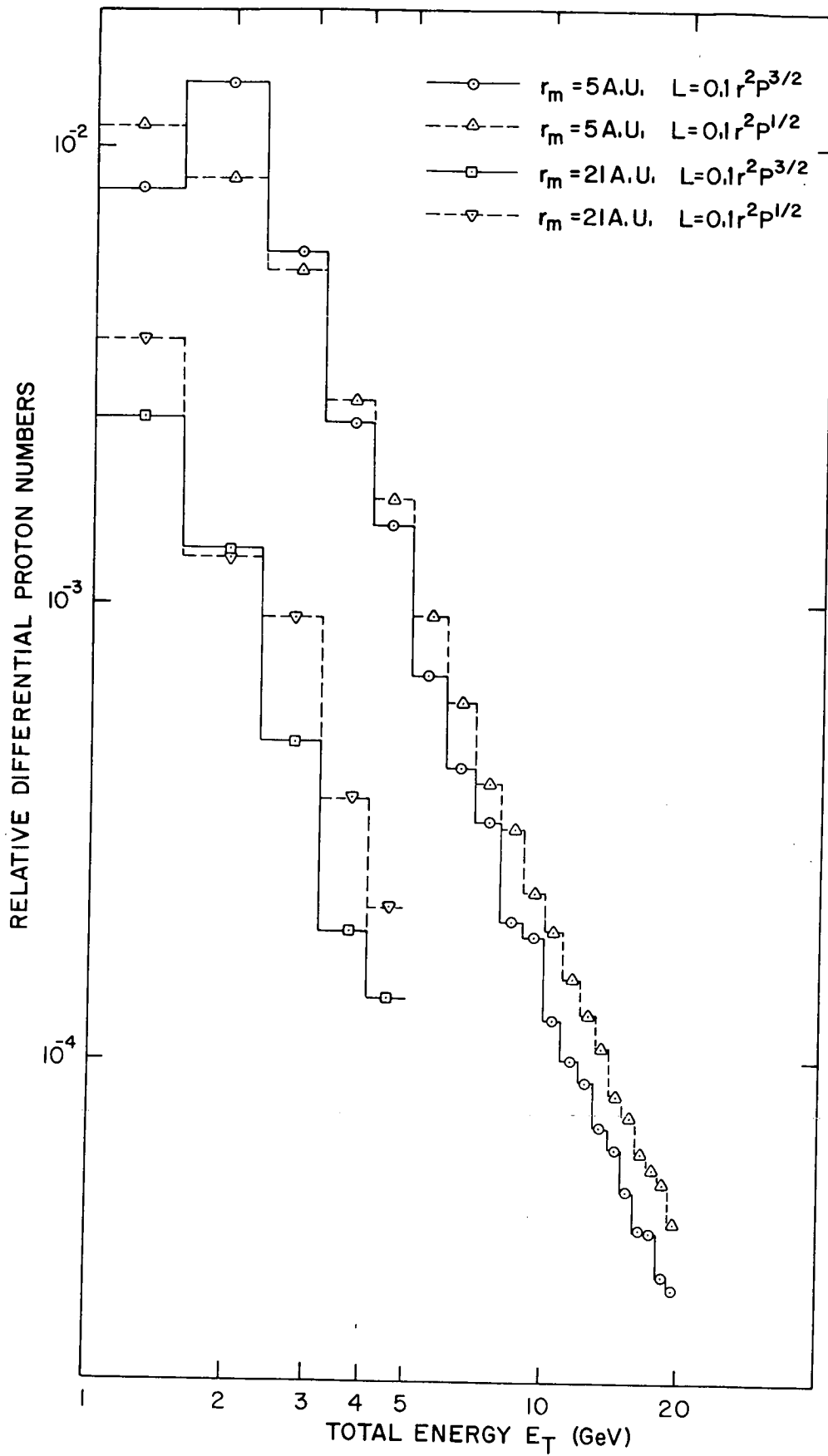


Figure 4

